PCCP

PAPER

View Article Online
View Journal | View Issue

Cite this: *Phys. Chem. Chem. Phys.*, 2017, **19**, 23809

Self-assembled mesoscopic surface domains of fluorocarbon–hydrocarbon diblocks can form at zero surface pressure: tilting of solid-like hydrocarbon moieties compensates for cross-section mismatch with fluorocarbon moieties†

Christian Schwieger,[a] Xianhe Liu[b] and Marie Pierre Krafft *[b]

Received 14th April 2017,
Accepted 30th May 2017

DOI: 10.1039/c7cp02432k

rsc.li/pccp

At low molecular areas, fluorocarbon–hydrocarbon diblocks ($C_nF_{2n+1}C_mH_{2m+1}$, *FnHm*), when spread as Langmuir monolayers on water, form organized monodisperse circular self-assembled domains, one molecule high and tens of nanometers in diameter. Whether such domains form at high molecular areas (low surface pressures) could until now not be established. Furthermore, the common assumption was that the inner core hydrocarbon chains within these domains were in the liquid state in order to compensate for the difference in the cross-section area between the perfluoroalkyl ($\sim$30 Å^2) and alkyl ($\sim$20 Å^2) chains. Our IRRAS investigation of *F8H16* now establishes (1) that these diblock surface domains do exist at the air/water interface at large molecular areas (zero surface pressure), (2) that they remain essentially unchanged throughout film compression, and (3) that the *H16* moieties are actually stretched in an all-*trans* configuration and tilted by $\sim$30° with respect to the normal to the monolayer in order to satisfy the greater space requirement of the *F8* moieties. Consequently, the core of the domains is in an ordered, crystalline-like state, and the domains can be visualized as solid particles at the air/water interface.

1 Introduction

$C_nF_{2n+1}C_mH_{2m+1}$ (*FnHm*) diblocks are highly hydrophobic amphiphilic, amphisteric and amphidynamic molecules that display a marked propensity for self-assembly, nanocompartmentation and nanostructuration.[1,2] They form stable Langmuir films on water in spite of the absence of polar heads.[3] They also form dense films at the hydrocarbon/fluorocarbon interface (surface freezing).[4] In their bulk solid state they form fibers, liquid crystals and gels.[5–7] They can also be used as film and shell components for modifying and controlling the film phase behavior, emulsion stability, liposome stability and permeability, and fiber formation.[8–11]

When compressed on the surface of water or deposited on solid surfaces these diblocks form sturdy ordered arrays of circular monodisperse surface domains.[1,2] It was shown that the *Fn* segments extend toward the air phase while the *Hm* segments are oriented toward the water phase or the solid surface. A first essential open question concerned the existence of these surface domains at large molecular areas, that is, when the molecules are not subjected to lateral pressure. A second open question concerned the conformation and ordering of the alkyl (*Hm*) moieties within the surface domains. The latter question arises because of the difference in the cross-section areas between the two moieties: 27–30 Å^2 for the *Fn* segment *versus* 18–21 Å^2 for the *Hm* segment.[1] In order to compensate for this difference in space demand when diblocks are closely packed, it has generally been presumed that the *Hm* moieties would adopt a disordered liquid state while the *Fn* moieties would be in a solid (crystallized) state (Scheme 1a). This had, however, never been established and was still a matter of debate. Examples of papers that have suggested disordered (liquid-like) *H*-blocks include, in the solid state,[12–16] and in Langmuir films.[17–19,20–23] An alternative hypothesis would be that the *Hm* moieties are tilted respective to the normal to the interface, while the *Fn* moieties are, except near the edges, close to normal to this interface (Scheme 1b). The limiting diameter of the *F8H16* nanodomains was calculated to be 26 nm for a dislike model.[2] A previous theoretical paper showed that the

---

[a] Institute of Chemistry, Martin-Luther University Halle-Wittenberg, D-06099 Halle (Saale), Germany

[b] Institut Charles Sadron (CNRS), University of Strasbourg, 23 rue du Loess, F-67034 Strasbourg, France. E-mail: krafft@unistra.fr

† Electronic supplementary information (ESI) available: Sets of experimental and simulated IRRA spectra in the OH and CH_2 stretching vibrational range recorded at different compression states. See DOI: 10.1039/c7cp02432k

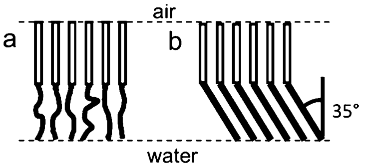

Scheme 1 Two ways of compensating for the difference in the cross-section between the *F*8 (open bars) and *H*16 moieties (solid lines): (a) adopting a liquid state for the *H*16 moieties, or (b) tilting extended all-*trans* *H*16 moieties by about 35° with respect to the surface.

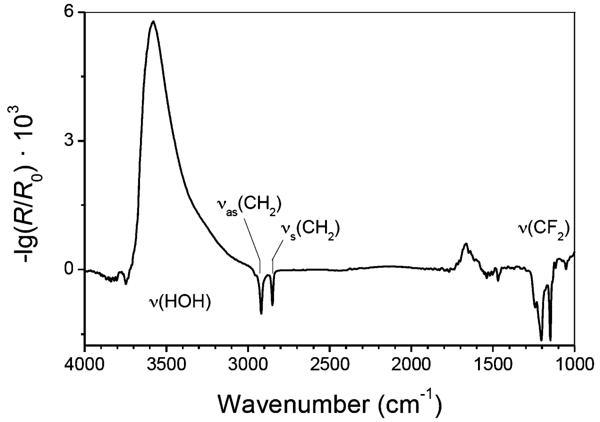

Fig. 1 IRRA spectrum of *F*8*H*16 recorded in s-polarization and at an angle of incidence of $\varphi = 60°$. It is calculated according to $RA = -\lg(R/R_0)$, R and R_0 being the sample and reference reflectivity spectra, respectively. The presented spectrum is an average of 10 individual spectra measured in the area range of 30 to 10 Å^2 molecule^{-1}. The most prominent bands used for the analysis of the interfacial film are marked. They include ν(HOH): stretching vibrations of the water subphase; $\nu_{as}(CH_2)$ and $\nu_s(CH_2)$: antisymmetric and symmetric CH_2 stretching vibrations of the alkyl block, respectively; $\nu(CF_2)$: CF_2 stretching vibrations of the perfluoroalkyl block.

limiting diameter was determined by the electrostatic activation energy (energy barrier for nanodomain fusion).[23] The predicted kinetically controlled nanodomain size was in the 24–32 nm range. Both values are in agreement with the experimental results.

We undertook to resolve these questions using Langmuir and Langmuir–Blodgett film techniques, infrared reflection–absorption spectroscopy (IRRAS) and atomic force microscopy (AFM). When applied to Langmuir films, IRRAS monitors vibrational frequencies and intensities of molecules or molecular moieties at the air/water interface. It allows investigation of the organization and orientation of a self-organized film at a sub-molecular level. Vibrational frequencies are sensitive to the organization (*e.g.* conformation, state of binding) of the vibrator.[24–28] In particular, the frequencies of the CH_2 stretching vibrations differ in the liquid condensed (LC) and the liquid expanded (LE) phase of lipid monolayers.[29–31] The intensities of vibrational bands are sensitive to the orientation of the transition dipole moment (TDM) with respect to the incoming IR beam. The intensity of the CH_2 stretching vibration depends on the orientation of the stretched alkyl segment with respect to the incoming IR light electrical field vector. Thus, variations in the angle of incidence (φ) and of the polarization (parallel, p or perpendicular, s) of the IR light beam can be used to determine the orientation of the alkyl chain.[31–33] Similarly, the average layer thickness can be determined from the angle and polarization dependency of the intensity of the OH stretching vibrational bands, originating from the water subphase.[34] Simultaneous measurements of the IRRA spectra and Langmuir isotherms enable correlating the structural and orientational changes of molecules in the monolayer with accidents occurring in the isotherms, such as "kinks" or plateaus. The vibrational bands that we analyzed are indicated in the IRRA spectrum shown in Fig. 1.

Semi-fluorinated carboxylic acids $C_nF_{2n+1}(CH_2)_mCOOH$ (n = 4, 6, 8; m = 22) that form surface domains when spread and compressed on an aqueous lanthanum acetate subphase and transferred onto silicon wafers were studied using polarization modulation infrared reflection absorption spectroscopy (PM-IRRAS).[35,36] The hydrocarbon segment was shown to be both tilted by $\theta \sim 40–43°$ and twisted ($\psi \sim 61–66°$) on water, and less tilted ($\theta \sim 29–34°$) and twisted ($\psi \sim 50–52°$) once transferred on a solid surface. The objective was actually to probe the effect of temperature on the fusion of the surface domains. No attempt was made to probe the existence of surface domains at large molecular areas and the conformation of the carboxylic acids. GISAXS performed on a series of *FnHm* diblocks allowed clear-cut determination of the existence, size and organization of surface domains for molecular areas below 30 Å^2, that is, in the area range for which the surface micelles are in close contact and are organized in a hexagonal array.[37] For higher molecular areas, GISAXS signals were not detected, meaning that either the surface domains do not exist or that they are disordered on the surface of water. IRRAS allowed us to determine the organization of the alkyl chains of *FnHm* at different compression states, the alkyl chain tilt angle with respect to the monolayer's surface, and the thickness of the layer. An all-*trans* conformation would indicate that the alkyl chains are in van der Waals contact, that is, orderly arranged within domains.

Spatial organization of the domains is not necessary to conclude on their existence and internal organization. So far, isolated domains at large surface areas have only been identified after transfer on silica wafers.[38]

Whether these organized domains exist at a large molecular area is relevant to the mechanisms of their formation. Our data now establish that surface domains do already exist at large molecular areas, that is, even when the domains are not part of an ordered array on the surface of water, and that compression does not modify the order of the diblocks within the surface domains. We also found that within these domains, and contrary to common belief, the *Hm* segments are crystallized in an all-*trans* conformation and are tilted with respect to the surface's normal.

2 Experimental

2.1 Materials

*F*8*H*16 was synthesized according to ref. 39 and purified by repeated crystallizations from methanol. Chemical purity

(> 99%) was determined by TLC, NMR, elemental analysis and MALDI-TOF mass spectrometry. Spreading solutions of *F8H*16 (2 or 4 mmol L^{-1}) were prepared in analytical grade chloroform (Aldrich). Water was purified using a Millipore system (surface tension: 72.1 mN m^{-1} at 20 °C; resistivity: 18.2 MΩ cm). The length of the fully extended *F8H*16 diblock was calculated to be 3.39 nm, using the formula $l = 1.306$ Å $n + 1.265$ Å $m + 3.26$ Å, with *n* and *m* being the number of fluorinated and hydrogenated carbons, respectively.[14]

2.2 Compression isotherms

Surface pressure *versus* molecular area (π/A) isotherms were recorded on a Langmuir trough (NIMA Technology, Coventry, UK) equipped with two movable barriers. The area available for the monolayer was controlled by two symmetrically movable barriers and is expressed as the molecular area (*A*) in units of $Å^2$ $molecule^{-1}$. The surface of the trough was 240 cm^2. The surface pressure was measured using the Wilhelmy plate method. 25 μL of *F8H*16 solution (1.5 mg mL^{-1}, $CHCl_3$) were spread on the surface of water and 10 min were allowed for solvent evaporation. Variation of the compression speed from 2 to 10 cm^2 min^{-1} did not affect the isotherms significantly. Compression speed was kept at 5 cm^2 min^{-1} (1 $Å^2$ min^{-1} $molecule^{-1}$). Temperature was regulated at 20 ± 0.5 °C. Each experiment was run at least 3 times. Experimental errors were ±0.5 mN m^{-1} on the surface pressure values and ±1 $Å^2$ on the molecular area values.

2.3 Langmuir–Blodgett films

The *F8H*16 films were compressed up to the desired surface pressure and transferred at constant pressure onto silicon wafers previously treated with a Plasma Cleaner (Harrick Plasma, Ithaca, NY; medium intensity), using the Langmuir–Blodgett technique (one monolayer transferred; lift speed: 2 mm min^{-1}).

2.4 AFM

The transferred films were analyzed by Multimode AFM (NanoScope IV Controller, Digital Instruments, Santa Barbara, CA) in tapping mode. The cantilever (Olympus) was fitted with a 3–10 nm tip. The resonance frequency and the spring constant were 300 kHz and 40 mN m^{-1}, respectively. At least three different samples were analyzed, and several positions were scanned on the wafer for each sample. The error on measurements along the *z*-axis was estimated to be ±0.5 nm. The surface domain size characteristics (mean diameter, mean height) and their surface coverage were determined using the Nanoscope image treatment software.

2.5 IRRAS measurements

IRRAS measurements were performed using a Bruker Vertex 70 FT-IR spectrometer equipped with the A511 reflection unit (Bruker Optics, Germany) to guide the IR beam to the air/water interface as well as the reflected beam to an external MCT detector cooled with liquid nitrogen. The angle of incidence (φ) was varied between 26° and 70° by increments of 4° and the polarization of the IR beam was set to parallel (p) or perpendicular (s) with respect to the plane of incidence at each probed φ by means of a wire grid polarizer. The size of the IR beam at the point of reflection was 0.55–1.5 cm^2, depending on φ. The spectrometer and reflection unit were purged with dry air to reduce water vapor absorption bands. In addition, the reflection unit and Langmuir trough were placed into a closed Plexiglas container in order to maintain a stable atmosphere. 1000 or 2000 scans were averaged in s or p-polarization, respectively. The spectra were recorded with a resolution of 4 cm^{-1}. The resolution was improved by a zero filling with a factor of 2 before Fourier transformation using Blackman–Harris apodization, resulting in an apparent resolution of 2 cm^{-1}. The Langmuir trough system (Riegler and Kirstein GmbH, Germany) consisted of a rectangular sample trough (30 × 6 cm^2) and a circular reference trough (r = 3 cm). Both troughs were thermoregulated at 20 °C by a circulating water bath. Sample and reference troughs were filled with the same subphase (H_2O), the level of which was controlled by a laser beam reflected off the surface and kept constant by pumping water from external reservoirs. *F8H*16 was dissolved in chloroform and spread drop wise with a microliter syringe onto the water surface in the sample trough. After spreading, evaporation of the chloroform and formation of a homogeneous monolayer were allowed for 10 min. The surface pressure was detected using a Wilhelmy pressure sensor plate. The trough system was mounted on a shuttle allowing measurement of either the reference (R_0) or sample (R) reflectivity spectra. The reflectance–absorption spectra were then calculated according to $RA = -\lg(R/R_0)$. Angle and polarization dependent measurements were done in triplicate and averaged before analysis.

2.6 IRRA spectral simulations and fitting

IRRA spectra were simulated and fitted to the experimental spectra using a program written in MATLAB. For IRRA spectral simulations we adopted the 3-layer model of Kuzmin *et al.*[40] using the method of calculation of multiple bands described by Schwieger *et al.*[34] The optical constants (refractive index, *n* and absorption coefficient, *k*) of the aqueous subphase were used as reported.[41] The refractive index of the alkyl layer was set to $n_H = 1.41$[32] and that of the perfluoroalkyl layer to $n_F = 1.31$ (own results, details will be published separately). For simulations of a closely packed *FnHm* layer, an averaged refractive index weighted by the fluorocarbon and hydrocarbon volume fractions was used, according to:

$$n = n_F \cdot \nu_F + n_H \cdot \nu_H \tag{1}$$

which results in $n = 1.37$ for *F8H*16, using $\nu_F = 0.44$ and $\nu_H = 0.56$, respectively. A more loosely packed monolayer containing void area has a lower average refractive index. The polarizer quality was set to $\Gamma = 0.007$ (0.7% transmittance of s-polarized light, while the polarizer was set to p-polarization).

Simulated spectra were fitted to the measured spectra by a non-linear least square fit using the Levenberg–Marquardt algorithm. Spectra measured at all probed φ and polarizations were simultaneously fitted with the same parameters. Spectra measured at $46 \leq \varphi \leq 58°$, close to the Brewster angle, were omitted from the analysis. The fit was performed in two steps: (i) the OH stretching vibrational bands were fitted in the range of 3000–3650 cm^{-1}, with the layer thickness d and the refractive index n being the only adaptable parameters. (ii) The symmetric and antisymmetric CH_2 stretching vibrational bands were simultaneously fitted in the range of 2910–2930 cm^{-1} and 2840–2860 cm^{-1}, respectively. d and n were used as determined in step (i). n was used as calculated by formula (1). The polar angle α (the angle between the TDM and the alkyl chain main axis) was set to 90° for both vibrations. The polar angle β between the TDM and the alkyl chain minor axis (perpendicular to the main axis and in the plane of the C atoms) was set to 0° and 90° for the symmetric and antisymmetric stretching vibrations, respectively. The absorption coefficients (k_{max}), the bandwidth (full width at half maximum, fwhm) and the orientational angles (tilt, θ: the angle between the alkyl chain main axis and the surface normal; and twist, ψ: rotation of the alkyl chain about its main axis) were free fitting parameters.

3 Results and discussion

3.1 Identification of surface domains at large molecular areas

The *F8H*16 monolayer exhibits a monotonous compression isotherm characterized by a limiting molecular area A_0 of ~31–32 Å², which corresponds to the cross-section of a perfluoroalkylated chain (Fig. 2). The collapse pressure π_{coll} of the monolayer is ~12 mN m^{-1}, as reported previously.[37,42] Further compression leads to the formation of multilayers.[43] The minor peak appearing in the compressibility curve at 31.5 Å² is likely due to a relaxation in the packing of the nanodomains. This phenomenon is currently under investigation. The isothermal compressibility coefficient Cs of the *F8H*16 monolayer was calculated from the $\pi - A$ isotherm according to $Cs = (-1/A)(dA/d\pi)$, where A is the area per molecule and π the surface pressure. The minimum compressibility value, Cs_{min}, is 5.0×10^{-3} m mN^{-1}, in line with previous reports.[42] The compressional modulus (the reciprocal quantity of Cs) Cs^{-1} is ~200 mN m^{-1}, indicating that the *F8H*16 monolayer is in an LC state.

Fig. 3a shows an AFM image of a *F8H*16 monolayer transferred on a silicon wafer at a molecular area of ~60 Å² (zero surface pressure). The images clearly show that surface domains are present. The surface area occupied by the domains is 52 ± 2%, as determined by the Nanoscope image treatment software. This value is in good agreement with the theoretical value (50–57% in the 60–53 Å² molecular area range). Although the surface pressure is no longer maintained during transfer, which likely modifies the interactions between the surface domains, these interactions are strong enough to maintain the surface domains on the substrate. The surface domains' mean diameter is 32 ± 2 nm (Fig. 3b), that is, similar to the diameter of surface domains when directly measured on the surface of water[37] or transferred at high pressure onto a silicon wafer.[42] Distortion effects due to convolution with the AFM tip shape that often lead to an overestimation of the sizes are not an issue here. The height of the surface domains is 3.0 ± 0.1 nm, that is, significantly smaller than the extended molecular length (3.39 nm).

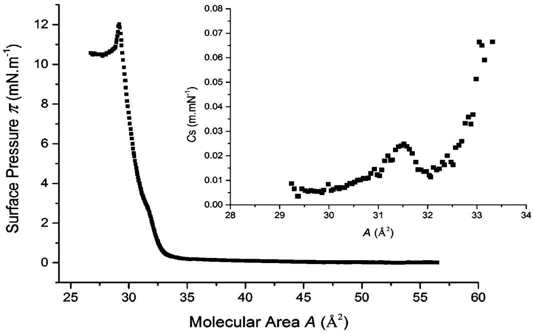

Fig. 2 Variation of surface pressure (π) and compressibility (Cs, inset) *vs.* molecular area (A) obtained by compressing *F8H*16 at the air/water interface at 20 °C.

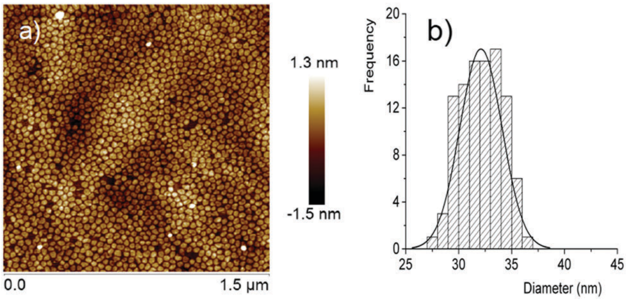

Fig. 3 (a) Height AFM image of the *F8H*16 LB films transferred on silicon wafers at 0 mN m^{-1} ($60 < A < 53$ Å²); (b) Histogram of surface domain diameters as assessed by image analysis of (a).

3.2 Alkyl chain conformation

Fig. 4 is a plot of the wavenumbers of the CH_2 antisymmetric ($\nu_{as}(CH_2)$) and symmetric ($\nu_s(CH_2)$) stretching vibrations of *F8H*16 as a function of molecular area. The position of these vibrations is indicative of the conformation of the alkyl chain. For comparison purposes, the corresponding wavenumbers of a typical phospholipid (dipalmitoylphosphatidylcholine, DPPC)

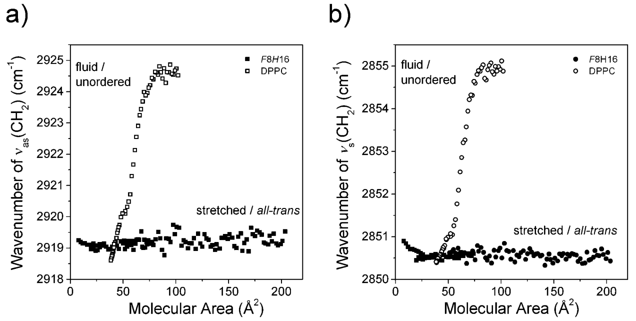

Fig. 4 Positions of the (a) antisymmetric and (b) symmetric CH_2 stretching vibrational bands in Langmuir films of *F8H*16 (full symbols) and DPPC (open symbols) at the air/water interface at different compression stages. The IRRA spectra were recorded with s-polarized light at an angle of incidence of φ = 60°.

are added in the figure. In the case of DPPC, the decrease in wavenumbers observed when the molecular area decreases is typical of a liquid expanded (LE)/liquid condensed (LC) (*i.e.* disordered/ordered) phase transition occurring upon compression, which goes along with a decrease in the number of *gauche* conformations per alkyl chain.[30,44]

Band positions below 2920 cm^{-1} and 2851 cm^{-1} for $\nu_{as}(CH_2)$ and $\nu_s(CH_2)$, respectively, are typical of alkyl chains in fully stretched all-*trans* conformation. In contrast, *F*8*H*16 is seen to vibrate consistently at the same low wavenumbers, independently of the available surface area and of surface pressure. This establishes that the alkyl segments of the *F*8*H*16 molecules are always in their fully stretched all-*trans* conformation, that is, remain highly organized throughout the compression experiment. This experiment provides strong evidence for self-aggregation into organized structures at the air/water interface even at high molecular areas.

In order to ensure that the vibration wavenumbers of the *H*16 moiety of *F*8*H*16 are comparable to those of other alkyl chains (*e.g.* in DPPC) and that the usual interpretation is valid, we measured the transmission IR spectra in different physical states: (i) in the crystalline state (*F*8*H*16 powder in the KBr tablet, the black line in Fig. 5) and (ii) in solution (in $CDCl_3$, the red line in Fig. 5). It is seen that the wavenumbers compare well with those of other alkyl derivatives.[44] This shows that the *Fn* moiety does not affect the vibration frequencies of the *Hm* moiety. The IRRA spectra recorded on Langmuir films at the air/water interface (Fig. 5, lower panel) compare well with the spectrum of crystalline *F*8*H*16, confirming that *F*8*H*16 is well organized at the interface at any probed molecular area. The data collected in Fig. 4 and 5 establish that the alkyl chains are in a crystalline state independently of molecular area. Even when the latter largely exceeds the area demand of one *F*8*H*16 molecule, that is, at 100 Å^2 or more, the vibrations are essentially identical to those recorded at 35 Å^2 or below, that is, when the surface domains are closely packed or evenly stacked in multilayer arrangements. This implies that the surface domains already form at the highest molecular area investigated and, conversely, that the *F*8*H*16 film is never in a gaseous or a liquid expanded state. Consequentially, compression leads only to bringing the already existing domains closer to each other.

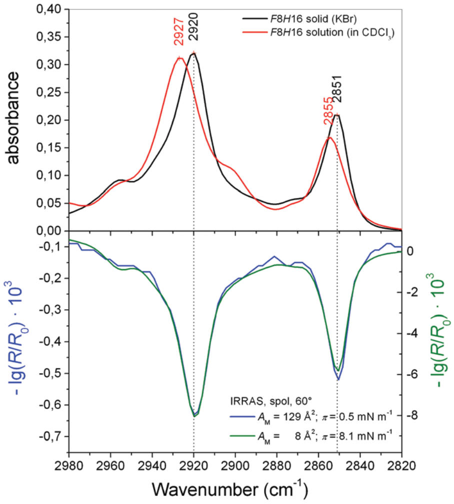

Fig. 5 Comparison of CH_2 stretching vibrational band positions of *F*8*H*16 in the solid state (black), in $CDCl_3$ solution (red), and when spread as a Langmuir film at the air/water interface in the expanded (blue) and compressed (green) states.

3.3 Angle and polarization dependent IRRAS measurements

From the IRRA band shape and intensity dependency on the angle of incidence φ of the IR beam and on its polarization, one can calculate the orientation of the vibrating molecular moieties if the direction of the corresponding transition dipole moment is known. Furthermore, the average layer thickness can be calculated from the angle and polarization dependency of the OH stretching vibration that comes from the aqueous subphase. In order to probe if the internal structure of the *FnHm* surface domains is influenced by their compression, we recorded the IRRA spectra while varying φ and polarization of the IR beam at various areas per molecule, and we determined (i) the alkyl chain tilt angle and (ii) the average layer thickness.

3.3.1 Alkyl block orientation. Fig. 6 presents angle and polarization dependent spectra of an *F*8*H*16 monolayer recorded at 40 Å^2 molecule^{-1}, together with the best fitting simulated spectra. All the spectra presented were fitted using one global non-linear least square fit, the order parameters (longitudinal, *S* and transversal, *D*) of the alkyl chain being the main fit parameters. These order parameters can be translated into the tilt angle θ (between the surface normal and the alkyl chain main axis) and the twist angle ψ (the rotation angle about the alkyl chain's main axis) as follows:[45–47]

$$S = \frac{3\langle\cos\theta\rangle^2 - 1}{2} \tag{2}$$

$$D = \left\langle \frac{3}{2}\sin^2\theta \cdot \cos 2\psi \right\rangle \tag{3}$$

These analyses allowed establishing that, at 40 Å^2 molecule^{-1}, the alkyl blocks of *F*8*H*16 are not perpendicular to the interface, but tilted by 30° and twisted by 90°. The same analysis was performed at other compression states, including at large molecular areas (see ESI† Fig. S1, S3, S5 and S7). The measured tilt and twist angles, as well as the corresponding order parameters, are collected in Table 1. Remarkably, the orientation of the alkyl chain *H*16 is essentially the same at all compression states. This indicates that the surface domains that are formed at high molecular areas already have the same internal structure as those obtained after compression is applied and close contact of the domains is reached. The tilting of the alkyl moiety allows compensation for the larger cross-sectional area of the perfluoroalkyl moiety. Given that the alkyl chains are in a stretched all-*trans* conformation, only tilting can bring them into van der Waals contact and prevents void volume. A tilting angle of θ = 35° would exactly compensate for the difference in cross-sectional areas when assuming circular cross-sections of 20 and 30 Å^2 for hydrocarbon and fluorocarbon chains, respectively.

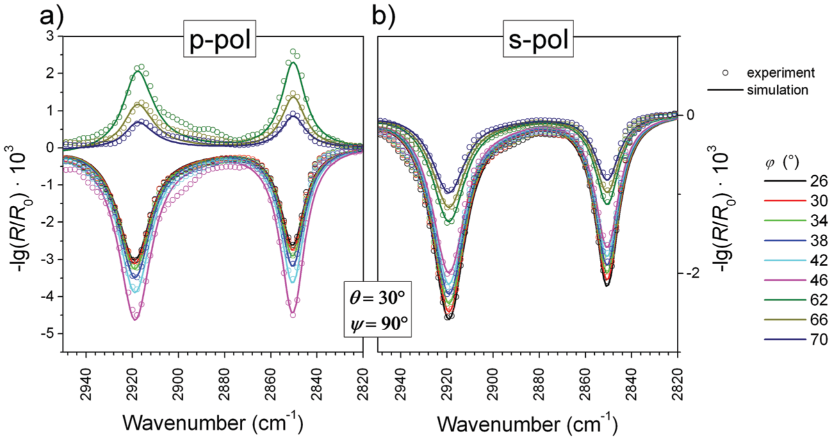

Fig. 6 Experimental (symbols) and best fitting simulated (lines) IRRA spectra of *F8H16* at 40 Å^2 molecule^{-1} in the range of the antisymmetric and symmetric CH_2 stretching vibrations. The spectra were recorded in (a) p-polarization and (b) s-polarization at different angles of incidence (φ) of the IR beam. All the spectra were fitted in one global fit with the same parameter. The best fit was achieved with an alkyl block tilt angle θ = 30° and a twist angle ψ = 90°.

Table 1 Parameters determined from the fitting angle and polarization dependent IRRA spectra of a *F8H16* film at different areas per molecule in the region of the OH stretching vibrations (average refractive index n, monolayer thickness d, extrapolated thickness that takes into account the non-uniformity of the monolayer d_{extr}) and CH_2 stretching vibrations (θ, ψ, S, D)

Area (Å^2 molecule^{-1})	n	d (nm)	d_{extr} (nm)	Tilt, θ (°)	Twist, ψ (°)	S	D
100	1.31	0.76	2.5	32	90	0.57	−0.42
80	1.31	0.94	2.5	31	90	0.61	−0.40
60	1.31	1.19	2.4	30	82	0.62	−0.36
40	1.37	2.23	3.0	30	90	0.62	−0.37
30	1.37	2.40	2.4	30	90	0.62	−0.37

The twist angle ψ (*i.e.* the non-zero transversal order parameter D) shows that the alkyl chains are not arranged in a uniaxial molecular symmetry. Rather, the tilting direction within the ordered domains is defined. This shows that the alkyl chains are arranged in a 2D crystalline lattice.

Whereas the tilt and twist angles are essentially the same for all probed areas, the determined refractive indices and extrapolated thicknesses vary slightly. The lower n values at higher areas per molecule can be attributed to a contribution of the bare water interface. The determination of d_{extr} might be hampered by averaging the refractive index over the covered and bare interface. The film might be affected by domain stacking at 30 Å^2 molecule^{-1} or by rearrangements occurring at such low areas (see the maximum in film compressibility in Fig. 2). Therefore, we think that the values of n and d_{extr} determined at 40 Å^2 molecule^{-1} are the most representative ones for a *F8H16* film organized in distinct surface domains. The good agreement with the other experimental values fully supports this assumption.

3.3.2 Layer thickness. An IRRA spectrum contains not only vibrations of the spread molecules but also non-compensated vibrations from the subphase. The thicker the interfacial film, the less compensated the vibrations and the more intense the signals. The thickness of the film as well as its refractive index were calculated from angle and polarization-dependent OH stretching vibrations of water in a fitting procedure as described in ref. 34. In Fig. 7, we show experimental and best fitting simulated spectra in the region of the OH stretching vibrations recorded from a *F8H16* film at 40 Å^2 molecule^{-1}. At 40 Å^2 molecule^{-1} the average layer thickness determined from the IRRAS band fit is 2.3 nm. However, at this area per molecule the domains are not yet in close contact and the surface film does not have a uniform thickness. Therefore, the determined average layer thickness contains contributions from void areas (empty water surface). However, assuming a constant molecular volume, the thickness can be extrapolated to the thickness that a uniform, close-packed surface layer (A_2) would have, according to:

$$V_{\text{m}} = A_1 \cdot d_1 = A_2 \cdot d_{\text{extr}} \tag{4}$$

This extrapolated thickness (d_{extr}) corresponds to the domain height at the probed molecular area (A_1).

From grazing incidence X-ray diffraction experiments it is know that at low surface areas the perfluorinated blocks of *F8H16* are arranged in a perpendicular hexagonal lattice within the surface domains.[48] Therefore, the molecular area of a putative completely covered surface layer of *F8H16* would correspond to the cross-sectional area of a CF_2 chain, *i.e.* 30 Å^2 molecule^{-1}.[1] Extrapolation of the fitted layer thickness d to this area gives a domain height of 3.0 nm. This value corresponds effectively to the domain height determined by X-ray reflectivity[22] and by AFM after transfer of the domains onto solid substrates (see above). Furthermore, this thickness is consistent with a model in which stretched alkyl segments of total length l = 2.1 nm are tilted by 30° while the perfluorinated segments are oriented perpendicular to the surface.

The tilted alkyl chains would then contribute to the layer thickness by $l \cdot \cos(\theta)$ = 1.9 nm and the perpendicular fluorocarbon chains by 1.2 nm, which adds up to a total height of 3.1 nm, essentially the same as was determined experimentally.

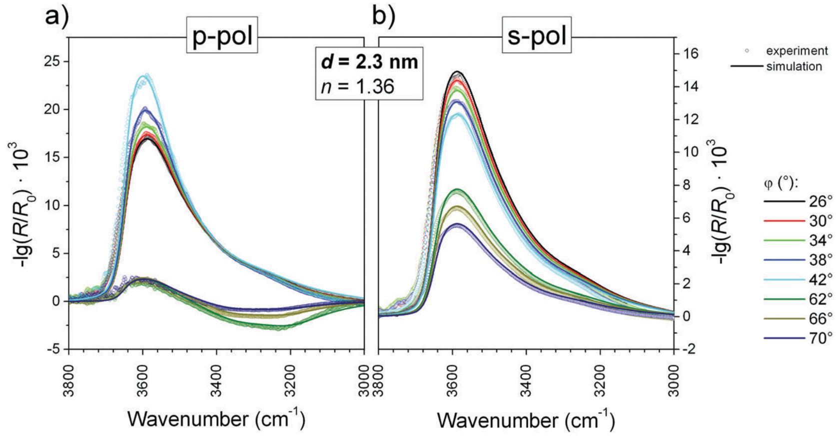

Fig. 7 Experimental (symbols) and best fitting simulated (lines) IRRA spectra of *F*8*H*16 at 40 Å^2 molecule^{-1} in the range of the OH stretching vibrations originating from the water subphase. The spectra were recorded in p-polarization (a) and s-polarization (b) at various angles of incidence (φ) of the IR beam. An average layer thickness d = 2.3 nm and an average refractive index n = 1.36 for the mixed hydrocarbon/fluorocarbon layer were determined by fitting the data.

Besides the layer thickness, the average refractive index of the interfacial film was a free fitting parameter. For a closely packed *F*8*H*16 layer at 30 Å^2 molecule^{-1}, we determined a value of n = 1.37. Interestingly, this corresponds to a theoretical predicted refractive index, calculated as volume weighted average of hydrocarbon (n_H = 1.41)[32] and perfluorocarbon (n_F = 1.31, own data) contributions. Average layer thicknesses and refractive indices determined at other areas per molecule are given in Table 1, and the corresponding spectra are shown in the ESI† (Fig. S2, S4, S6 and S8).

4. Conclusions

We have established by IRRAS investigations that, even at very high surface areas (zero surface pressure), self-assembled surface domains are formed when *F*8*H*16 is spread as a Langmuir film on the surface of water. The alkyl moiety *H*16 adopts a tilted orientation by 30° relative to the film's normal in order to compensate for the larger space requirement of the *F*8 moieties, which are normal to the surface of water. The internal structure of the surface domains is not affected by compression. We also establish that, contrary to earlier assumptions, the conformation of the alkyl moiety is not liquid-like. The alkyl core of the surface domains is crystalline and not disordered, independently of the molecular area. The determined alkyl chain twist angle shows that the alkyl chains are densely packed and that rotation about their long axis is hindered.

Acknowledgements

We thank the French Research Agency (grant ANR-14-CE35-0028-01) for funding this project (X. H. Liu PhD fellowship), the Groupement d'Intérêt Scientifique (GIS) Fluor (CNRS) for travel grants, and the ICS atomic force microscopy platform and Teclis Scientific (France) for technical support. C. S. thanks the Deutsche Forschungsgemeinschaft for financial support *via* grant FOR1145.

References

1 M. P. Krafft and J. G. Riess, *Chem. Rev.*, 2009, **109**, 1714–1792.
2 M. P. Krafft, *Acc. Chem. Res.*, 2012, **45**, 514–524.
3 G. L. Gaines, *Langmuir*, 1991, **7**, 3054–3056.
4 Y. Hayami and G. H. Findenegg, *Langmuir*, 1997, **13**, 4865–4869.
5 P. Lo Nostro, *Curr. Opin. Colloid Interface Sci.*, 2003, **8**, 223–226.
6 W. Mahler, D. Guillon and A. Skoulios, *Mol. Cryst. Liq. Cryst., Lett. Sect.*, 1985, **2**, 111–119.
7 J. Höpken and M. Möller, *Macromolecules*, 1992, **25**, 2482–2489.
8 S. Marie Bertilla, J.-L. Thomas, P. Marie and M. P. Krafft, *Langmuir*, 2004, **20**, 3920–3924.
9 M. P. Krafft, *Biochimie*, 2012, **94**, 11–25.
10 M. Schmutz, B. Michels, P. Marie and M. P. Krafft, *Langmuir*, 2003, **19**, 4889–4894.
11 M. P. Krafft, *J. Polym. Sci., Part A: Polym. Chem.*, 2006, **44**, 4251–4258.
12 C. Viney, T. P. Russel, L. E. Depero and R. J. Twieg, *Mol. Cryst. Liq. Cryst.*, 1989, **168**, 63–82.
13 P. Marczuk, P. Lang and M. Möller, *Colloids Surf.*, 2000, **163**, 103–113.
14 F. G. Tournilhac, P. Bassoul and R. Cortès, *Mol. Cryst. Liq. Cryst.*, 2001, **362**, 45–65.
15 F. A. Escobedo and Z. Chen, *J. Chem. Phys.*, 2004, **121**, 11463–11473.
16 M. Fujiwara, K. Satoh, S. Kondo and S. Ujiie, *Macromolecules*, 2006, **39**, 5836–5842.
17 Z. Huang, A. A. Acero, N. Lei, S. A. Rice, Z. Zhang and M. L. Schlossman, *J. Chem. Soc., Faraday Trans.*, 1996, **92**, 545–552.
18 N. Kim and S. Shin, *J. Chem. Phys.*, 1999, **110**, 10239–10242.
19 A. El Abed, E. Pouzet, M.-C. Fauré, M. Sanière and O. Abillon, *Phys. Rev. E: Stat. Phys., Plasmas, Fluids, Relat. Interdiscip. Top.*, 2000, **62**, R5895–5898.

20 M. P. Krafft, F. Giulieri, P. Fontaine and M. Goldmann, *Langmuir*, 2001, **17**, 6577–6584.

21 A. El Abed, M.-C. Fauré, E. Pouzet and O. Abillon, *Phys. Rev. E: Stat., Nonlinear, Soft Matter Phys.*, 2002, **65**, 051603.

22 M. Maaloum, P. Muller and M. P. Krafft, *Angew. Chem., Int. Ed.*, 2002, **41**, 4331–4334.

23 A. N. Semenov, A. Gonzàlez-Pérez, M. P. Krafft and J.-F. Legrand, *Langmuir*, 2006, **22**, 8703–8717.

24 R. G. Snyder, S. L. Hsu and S. Krimm, *Spectrochim. Acta*, 1978, **34A**, 395–406.

25 R. Mendelsohn, R. Dluhy, T. Taraschi, D. G. Cameron and H. H. Mantsch, *Biochemistry*, 1981, **20**, 6699–6706.

26 R. A. Macphail, H. L. Strauss, R. G. Snyder and C. A. Elliger, *J. Phys. Chem.*, 1984, **88**, 334–341.

27 L. K. Tamm and S. A. Tatulian, *Q. Rev. Biophys.*, 1997, **30**, 365–429.

28 D. L. Allara and R. G. Nuzzo, *Langmuir*, 1985, **1**, 52.

29 M. L. Mitchell and R. A. Dluhy, *J. Am. Chem. Soc.*, 1988, **110**, 712–718.

30 R. Hunt, M. L. Mitchell and R. A. Dluhy, *J. Mol. Struct.*, 1989, **214**, 93–109.

31 A. Blume and A. Kerth, *Biochim. Biophys. Acta*, 2013, **1828**, 2294–2305.

32 C. R. Flach, A. Gericke and R. Mendelsohn, *J. Phys. Chem. B*, 1997, **101**, 58–65.

33 R. Mendelsohn, G. R. Mao and C. R. Flach, *Biochim. Biophys. Acta, Biomembr.*, 2010, **1798**, 788–800.

34 C. Schwieger, B. Chen, C. Tschierske, J. Kressler and A. Blume, *J. Phys. Chem. B*, 2012, **116**, 12245–12256.

35 Y. Ren, K.-I. Iimura, A. Ogawa and T. Kato, *J. Phys. Chem. B*, 2001, **105**, 4305–4312.

36 Y. Ren, K.-I. Iimura and T. Kato, *J. Phys. Chem. B*, 2002, **106**, 1327–1333.

37 P. Fontaine, M. Goldmann, P. Muller, M.-C. Fauré, O. Konovalov and M. P. Krafft, *J. Am. Chem. Soc.*, 2005, **127**, 512–513.

38 A. Gonzàlez-Pérez, C. Contal and M. P. Krafft, *Soft Matter*, 2007, **3**, 191–193.

39 N. O. Brace, *J. Fluorine Chem.*, 1999, **93**, 1–25.

40 V. L. Kuzmin, V. P. Romanov and A. V. Mikhailov, *Opt. Spektrosk.*, 1992, **73**, 3–47.

41 J. E. Bertie and Z. D. Lan, *Appl. Spectrosc.*, 1996, **50**, 1047–1057.

42 G.-F. Zhang, P. Marie, M. Maaloum, P. Muller, N. Benoit and M. P. Krafft, *J. Am. Chem. Soc.*, 2005, **127**, 10412–10419.

43 C. de Gracia Lux, J.-L. Gallani, G. Waton and M. P. Krafft, *Chem. – Eur. J.*, 2010, **16**, 7186–7198.

44 J. Tuchtenhagen, W. Ziegler and A. Blume, *Eur. Biophys. J.*, 1994, **23**, 323–335.

45 R. Kiefer and G. Baur, *Mol. Cryst. Liq. Cryst.*, 1989, **174**, 101–126.

46 E. H. Korte, *Mol. Cryst. Liq. Cryst.*, 1983, **100**, 127–135.

47 H. Binder and H. Schmiedel, *Vib. Spectrosc.*, 1999, **21**, 51–73.

48 M. P. Krafft and M. Goldmann, *Curr. Opin. Colloid Interface Sci.*, 2003, **8**, 243–250.